Anesthesiology 2008; 108:1037–46

Lung Injury and Recovery in a Murine Model of Unilateral Acid Aspiration

Functional, Biochemical, and Morphologic Characterization

Maria Amigoni, M.D., Giacomo Bellani, M.D.,† Margherita Scanziani, M.D.,* Serge Masson, Ph.D.,‡ Elisa Bertoli, M.D.,* Enrico Radaelli, D.V.M.,§ Nicolò Patroniti, M.D.,† Alessandro Di Lelio, M.D.,‖ Antonio Pesenti, M.D.,# Roberto Latini, M.D.‡*

Background: **Acid aspiration is a complication of general anesthesia. Most animal models developed to define its pathophysiology have focused on the acute (≤24 h) phase of the injury. The authors describe a model of acid aspiration allowing the study of this type of lung injury over time.**

Methods: **The authors instilled hydrochloric acid (0.1 M, 1.5 ml/kg) or normal saline in the right bronchus of mice. Lung injury was evaluated at 6 h, 12 h, 24 h, and 2 weeks by assessing arterial blood gases, respiratory system compliance, lung wet weight normalized by body weight, lung myeloperoxidase activity, and histology. Twelve hours and 2 weeks after injury, a computed tomography scan was obtained.**

Results: **In the hydrochloric acid group, arterial oxygen tension decreased ($P < 0.05$) at 12 and 24 h, whereas it recovered at 2 weeks; respiratory system compliance was lower both at 24 h and 2 weeks ($P < 0.05$). Lung weight increased at 12 and 24 h ($P < 0.05$). Myeloperoxidase activity peaked between 6 and 12 h. Computed tomography at 12 h showed that almost 30% of the injured lung was abnormally aerated. Although reduced, the abnormalities were still present at 2 weeks as confirmed by a fibrotic scar well evident at histologic examination.**

Conclusion: **The authors characterized a murine model of regional acid aspiration allowing long-term survival. Despite a partial recovery, at 2 weeks the injury persisted, with evidence of fibrosis and lung compliance reduction. This long-term, low-mortality model seems suitable for assessment of the effects of different therapies on lung injury and repair.**

ASPIRATION pneumonitis (AP) occurs as a consequence of pulmonary aspiration of the acid content of the stomach.[1] Patients with disturbed consciousness (*e.g.*, drug overdose, seizures, cerebrovascular accident, sedation, anesthetic procedures) are at risk for this event.[2–5] Specifically, it has been shown that pulmonary aspiration can complicate between 1:2,000 and 1:7,000 general anesthesia procedures, accounting for 10–30% of all deaths associated with anesthesia.[6]

The main injurious mechanisms of AP are an early injury to the alveolar epithelium associated to an acute alteration of endothelial permeability, directly caused by the low pH of the aspirated gastric secretions, and a delayed secondary phase involving neutrophilic infiltration.[7,8]

Aspiration pneumonitis substantially differs from aspiration pneumonia, the latter being an infectious process of the lung after the inhalation of colonized oropharyngeal materials. Although these must be considered as separate clinical entities, they often overlap and coexist.[1] Indeed, it has been shown that AP can enhance the pneumonic process after a bacterial infection.[9] The course of AP is extremely variable, ranging from the "silent aspiration" to the dramatic clinical picture of acute lung injury or acute respiratory distress syndrome, which carry a mortality rate as high as 40–60%.[10–12] In a recent prospective cohort study, more than 10% of acute lung injury cases were associated to a witnessed aspiration,[13] perioperative aspiration increasing indeed the risks of intensive care unit admission and mortality by four and eight times, respectively.[14]

Given its clinical relevance, the pathophysiology of AP has been extensively investigated in animal models. Most models, however, have been focused on the acute phase of the injury, and few studies have systematically examined the evolution of acid aspiration injury and its recovery.

The purpose of this study was to characterize a nonlethal murine model of unilateral AP, from the acute phase to recovery over a 2-week time span.

Materials and Methods

Animals

Female CD-1 mice (22–28 g) were obtained from Charles River Laboratories (Lecco, Italy) and maintained under standard laboratory conditions. Procedures involving animals and their care were conducted in conformity with the institutional guidelines complying with national (D.L. n. 116, G.U., suppl. 40, 18 Febbraio 1992, Circolare n. 8, G.U., 14 Luglio 1994) and international laws and policies (EEC Council Directive 86/609, OJ L 358,1, December 12, 1987; *Guide for the Care and Use of Laboratory Animals*, US National Research Council, 1996).

* Resident, † Research Fellow, # Professor of Anesthesia, Department of Experimental Medicine, University of Milano-Bicocca and Department of Perioperative Medicine and Intensive Care, San Gerardo Hospital, Monza, Italy. ‡ Research Scientist, Department of Cardiovascular Research, Istituto di Ricerche Farmacologiche Mario Negri, Milan, Italy. § Research fellow, Department of Veterinary Pathology, Hygiene and Public Health, Section of Veterinary and Avian Pathology, Faculty of Veterinary Medicine, University of Milan, Milan, Italy. ‖ Chairman, Department of Radiology, San Gerardo Hospital, Monza, Italy.

Received from the Department of Experimental Medicine, University of Milano-Bicocca, Monza, Milan, Italy, and Istituto di Ricerche Farmacologiche Mario Negri, Milan, Italy. Submitted for publication June 27, 2007. Accepted for publication February 13, 2008. Supported by Ministero dell'Università e della Ricerca Scientifica, Rome, Italy, and Istituto di Ricerche Farmacologiche Mario Negri, Milan, Italy. Presented in part at the 19th Annual Congress of the European Society of Intensive Care Medicine, Barcelona, Spain, September 25–27, 2006.

Address correspondence to Dr. Pesenti: Department of Perioperative Medicine and Intensive Care, San Gerardo Hospital, Via Donizetti 106, 20052 Monza, Italy. antonio.pesenti@unimib.it.

Mice were randomly assigned to one of the study groups: lung injury with instillation of 0.1 M hydrochloric acid (HCl; pH 1) or sham with lung instillation of 0.9% saline.

General Experimental Protocol

Animals were anesthetized with a 400-mg/kg intraperitoneal injection of 2.5% Avertin® (Tribromoethanol; Sigma-Aldrich, Milan, Italy), orotracheally intubated with a 22-gauge angiocatheter, and ventilated with tidal volume of 8–10 ml/kg, respiratory rate of 130 min^{-1}, positive end-expiratory pressure of 2.5 cm H_2O, and fraction of inspired oxygen (F_{IO_2}) of 1. A 26-gauge plastic cannula was then introduced into the right bronchus through a small tracheal incision. Through this cannula, 1.5 ml/kg HCl, 0.1 M (HCl group), or 0.9% saline (NaCl group) was instilled. The bronchial catheter was removed, and the tracheal incision sutured with a 7-0 Ethicon suture (Rome, Italy). During instillation and for the next 10 min of mechanical ventilation, the animals were kept in a reverse Trendelenburg position (45°) and tilted to the right side (45°) to confine the instilled fluid to the right lung. Mechanical ventilation was stopped 10 min after instillation, and the mice were extubated and placed in an oxygenated chamber (F_{IO_2} 0.5) until full awakening.

Assessment of Injury

Animals were studied at 6 h, 12 h, 24 h, and 2 weeks after intrabronchial instillation of HCl or NaCl. Because most procedures to assess injury imply animal sacrifice, different animals were used at each time point. All of the study procedures described below were also performed in an untreated control group of mice to obtain baseline values.

Arterial Blood Gases and Myeloperoxidase Assay. After intraperitoneal injection of 2.5% Avertin® (400 mg/kg), mice were reintubated and mechanically ventilated (tidal volume, 8–10 ml/kg; respiratory rate, 130 min^{-1}; and F_{IO_2}, 0.21). After opening the chest, blood was sampled (0.5 ml) from left ventricle and analyzed (0.1 ml) with an I-STAT 1 portable analyzer (Oxford Instruments S.M, Burke e Burke, Menfis Biomedica, Milan, Italy). Peripheral total leukocytes were counted in 20 μl EDTA anticoagulated blood using an hemocytometer. The animals were then killed with an additional lethal dose of Avertin®, and the lungs were removed *en bloc* for determination of myeloperoxidase activity. After excision, lungs were separately weighed (Europe 500 balance; Gibertini, Milan, Italy). Lung wet weight/mouse body weight ratio was used to evaluate the presence of edema after instillation of HCl or NaCl.[15]

The lungs were washed with sterile saline, blotted dry, weighed, and homogenized in 0.5% hexadecyltrimethylammonium bromide in 50 mM phosphate buffer (pH = 6.0; 1 ml hexadecyltrimethylammonium bromide/100 mg tissue). The homogenate was sonicated twice, frozen, and then centrifuged at 12,000*g* for 15 min at 4°C, and myeloperoxidase activity was assayed according to the method of Goldblum *et al.*,[16] modified as follows: 50 μl homogenate was added with 1,405 μl phospate buffer, 50 mM; 30 μl hydrogen peroxide, 0.03%; and 15 μl *O*-dianisidine dihydrochloride, 16.7 mg/ml (Sigma-Aldrich, Milan, Italy). Absorbance at 460 nm was read every 15 s for 1 min.

Pressure–Volume Curve Assessment. The animals were killed with sodium pentobarbital (200 mg/kg intraperitoneal); the tracheotomy was reopened, and the trachea was cannulated with a 20-gauge angiocatheter fixed with a suture. A recruitment maneuver to 30 cm H_2O for 30″ was performed in all animals. Starting from functional residual capacity, while recording airway pressure (Gould Inc., Valley View, OH), three steps of inspiratory volumes were delivered, by a micro injection pump (CMA/100; Carnegie Medicine, Stockholm, Sweden), to a total volume of 0.9 ml. At each insufflation step, we allowed enough time to reach a stable plateau pressure. For each step, we calculated the ratio between the insufflated volume and the plateau pressure. Then the three values were averaged to obtain the static compliance of the respiratory system, which was normalized by the mouse body weight (C_{stat}).

Histologic Preparation and Examination. In the animals undergoing pressure–volume curve measurements, after this procedure, the abdomen was opened, the vena cava was sectioned, and the lungs were excised, weighed, and subjected to histologic procedures. For histologic examination, lungs were fixed in 4% paraformaldehyde for 24 h (at a pressure of 20 cm H_2O for the first 30 min) and then paraffin embedded and sectioned.

To quantify lung tissue damage, 5- and 10-μm transverse sections 200 μm apart were obtained by cutting the lungs from apex to base and then stained with hematoxylin and eosin (Sigma-Aldrich).

The extent of fibrosis was evaluated in 10-μm sections stained with Sirius red (Sigma-Aldrich) and examined under polarized light.

Histopathologic examination was performed according to a previously described scale,[17] with minimal modifications. Three complete transverse sections (cranial, middle, and caudal) of lung were examined from each animal. In each section of the injured and of the contralateral lung, the following six pathologic findings were analyzed: alveolar serofibrinous exudate with hyaline membranes formation, alveolar hemorrhage, alveolar inflammatory cells, alveolar septa thickening, parenchymal necrosis, and fibrosis. Severity and extension of each pathologic finding were scored as follows: for severity: 0 (absent), 1 (mild), 2 (moderate), 3 (marked); and for extension: 0 (absent), 1 (>0% and ≤25%), 2 (>25% and ≤50%), 3 (>50%).

A mean score for each finding for each lung was derived and expressed as the product of extent and severity. Histopathologic evaluations were performed in a blinded fashion by an experienced pathologist (E.R.).

CT Imaging. Mice were anesthetized with an intraperitoneal injection of Avertin® (300–400 mg/kg), placed in the prone position and spontaneously breathing on the computed tomography (CT) table for lung scanning. CT scans were acquired by means of a clinical Philips Brilliance 16-slice multislice tomography (Philips Medical Systems, Amsterdam, The Netherlands), with the following acquisition parameters: 90 kV, 53 mA; images were reconstructed with a slice thickness of 0.8 mm and with a pixel size of 0.16 mm. By means of a specifically developed software, we manually outlined, on each image, the right and left lung's profile separately. In the control mice, the mode value (around −500 Hounsfield units [HU]) and the shape of the frequency distribution of voxel density are similar to the data obtained in mice by other authors using micro-CT scanners.[18] A reader, blinded to the mice's treatment and to the time of observation, identified and outlined contiguous areas of abnormal density likely to indicate a pathologic process. The mean density ($CT_{abn,mean}$) and the amount of tissue of each of the selected areas, expressed as percentage of the whole right lung weight ($CT_{abn,w}$), were computed.

Statistical Analysis

Data are expressed as mean ± SD. A level of $P < 0.05$ was considered significant. Two-way analysis of variance was used to evaluate the effects of treatment, time, and their interaction on the continuous variables. When statistical significance was reached, the Bonferroni *post hoc* test was used to compare the HCl and NaCl groups at each time point. One-way analysis of variance with the Dunnett multiple comparison test was used to compare HCl group variables at each time point with baseline values. Comparison of histologic score between groups was performed using the Mann–Whitney U test.

Statistics were performed using Graphpad Prism 4.0 for Windows (San Diego, CA).

Results

General Findings

Damage selectivity was confirmed by lung macroscopic examination and wet weight after the animals' euthanasia. Whenever the instillation involved the contralateral lung or both lungs or no visible acid injury was seen, the animal was excluded from analysis (approximately 5%).

Two-week mortality in the mice subjected to acid instillation was 24%. Death occurred mainly during the first 6 h, the first cause of death being a pneumothorax occurring a few minutes after acid instillation (during mechanical ventilation). In the NaCl group, the mortality rate was approximately 14% (not significantly different from the mortality of the HCl group). In the NaCl group, death occurred later (after 24 h) compared with the HCl group, and no signs of pneumothorax were evident.

Pulmonary Function

At 12 and 24 h, arterial oxygen tension (Pao_2) was significantly lower in the HCl group than in the NaCl group. After 2 weeks, Pao_2 recovered, and there was no difference between the HCl- and the NaCl-treated mice (fig. 1A). Arterial carbon dioxide tension ($Paco_2$) was significantly higher in the HCl group at 6 and 12 h (fig. 1B).

C_{stat} of the HCl group was significantly lower at 24 h and at 2 weeks compared with the NaCl group. At variance with gas exchange, C_{stat} of the HCl-treated mice did not recover over time (fig. 2).

Lung Injury

Global lung wet weight/mouse body weight ratio was significantly higher in HCl-treated mice at 12 and 24 h compared with NaCl-treated mice (9.4 ± 0.9 *vs.* 6.3 ± 0.6 mg/g at 12 h and 9.1 ± 1.2 *vs.* 6.4 ± 0.5 mg/g at 24 h; $P < 0.05$). In the acute phase, the right lung of HCl-

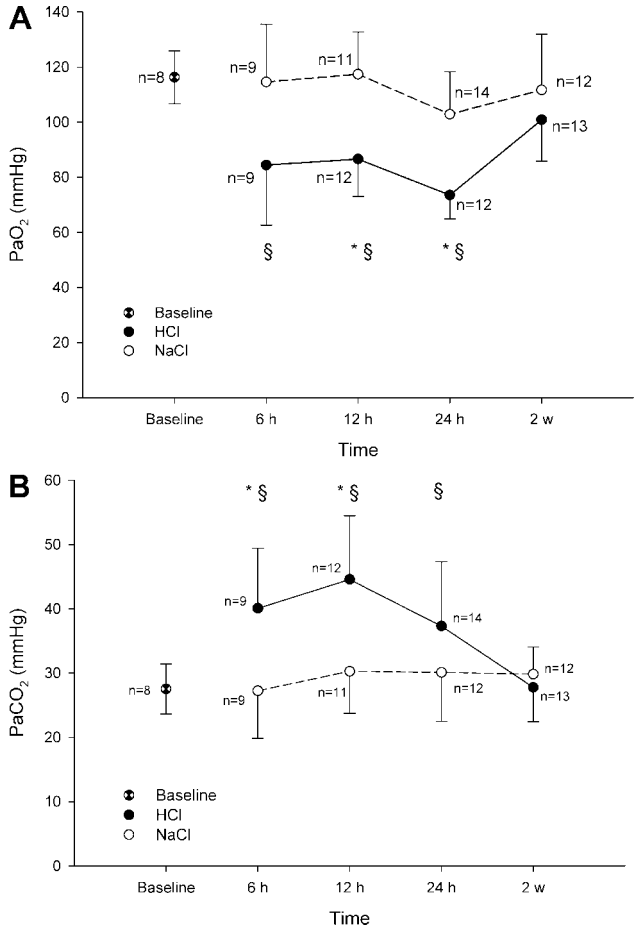

Fig. 1. Time course of gas exchange impairments for arterial oxygen tension (Pao_2; *A*) and arterial carbon dioxide tension ($Paco_2$; *B*). * $P < 0.05$ *versus* saline (NaCl) group at the corresponding time point. § $P < 0.05$ *versus* baseline, in hydrochloric acid (HCl) group.

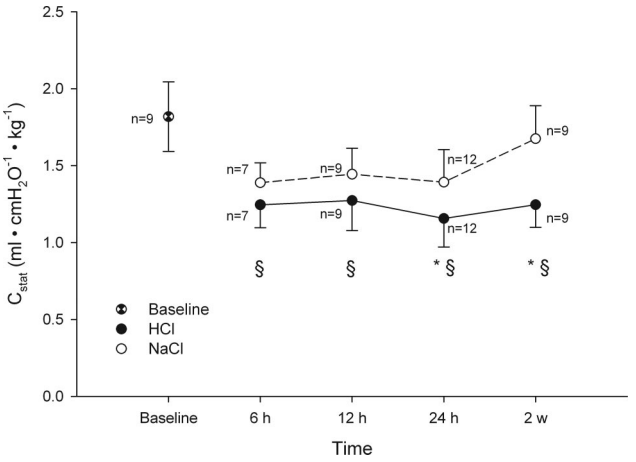

Fig. 2. Time course of static respiratory system compliance normalized by mouse body weight (C_{stat}). Pressure–volume curves were obtained by insufflating the lungs with 300 μl air three times to a total volume of 900 μl. For each step, compliance was calculated as the ratio between the insufflated volume and the plateau pressure. The three values were averaged to obtain C_{stat}. While at 6 h C_{stat} decreases similarly in the two groups, only in the saline (NaCl) group do the values improve over time. * $P < 0.05$ *versus* NaCl group at the same time point. § $P < 0.05$ *versus* baseline, in hydrochloric acid (HCl) group.

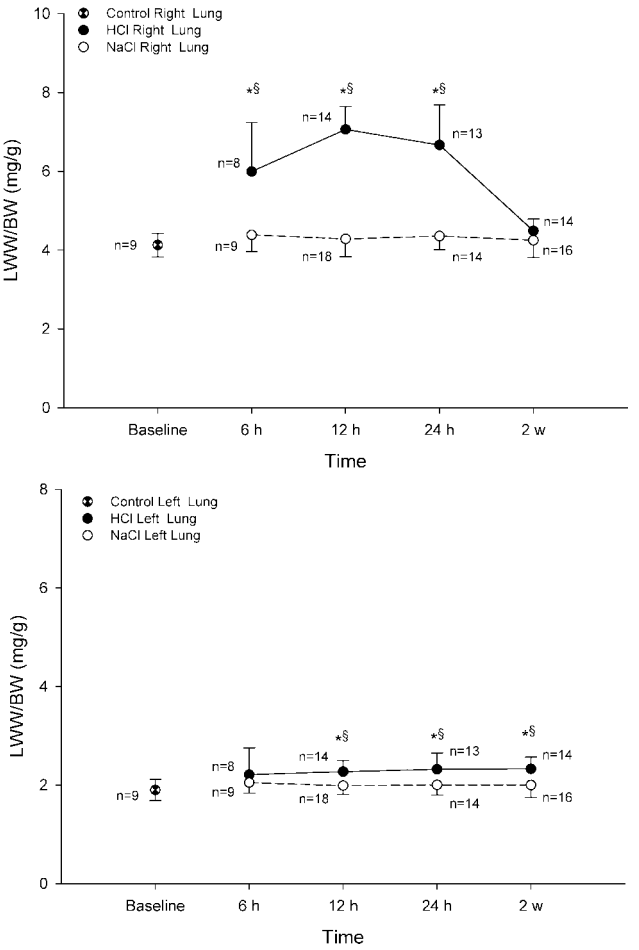

Fig. 3. Time course of lung wet weight normalized by mouse body weight (LWW/BW). * $P < 0.05$ *versus* saline (NaCl) group, ipsilateral lung at the same time point. § $P < 0.05$ *versus* baseline, in the hydrochloric acid (HCl) group.

treated mice showed a higher relative weight than that of the NaCl-treated ones, whereas in the contralateral lung, the difference between the two groups was smaller and relatively constant over time (fig. 3).

Myeloperoxidase activity, a marker of neutrophilic infiltration, increased significantly in both the HCl and NaCl groups (table 1). Six hours after HCl or NaCl administration, neutrophilic infiltration was increased both in the right and in the left lung. Although acid (and saline) was instilled into the right lung only, leukocyte trafficking was increased bilaterally, possibly indicating a decompartmentalization of the inflammatory response beyond the directly injured lung. In the NaCl group, however, myeloperoxidase activity substantially decreased toward baseline values at 12 h, whereas in the HCl group, it decreased more slowly, particularly in the right lung. The behavior of the peripheral blood leukocyte count was somehow delayed, reaching a peak in the HCl group at 12 h, going back to values not different from the NaCl group at 24 h (table 2).

Histologic Findings

Figure 4 and table 3 summarize the histologic findings for both the HCl and the NaCl group. The majority of the histopathologic changes described affected the right caudal pulmonary lobe. Six hours after HCl instillation, the dependent portion of that lobe was involved by coagulative necrosis. Diffuse acute inflammatory changes affected the adjacent vial parenchyma. In these areas, alveolar septa were expanded by capillary congestion and hemorrhage with sparse neutrophilic infiltration and protein-rich edema. Moderate amounts of intraalveolar serofibrinous exudation with scattered neutrophils and extravasated erythrocytes were also evident. At this stage, no pathologic changes were observed in the contralateral lung. Twelve hours after HCl instillation, a greater extent of bronchioalveolar serofibrinous exudation with hyaline membrane formation, a larger amount of intraalveolar and interstitial neutrophilic infiltration, and hemorrhage were noticed. Compared with 12-h lesions, 24 h after HCl instillation, a drastic increase in serofibrinous exudation, hyaline membrane formation, and bronchioalveolar infiltration of leukocytes (mostly neutrophils and foamy macrophages) and erythrocytes were observed. A widened perinecrotic hemorrhagic rim associated with prominent histioneutrophilic infiltration, cellular debris accumulation, and blood vessel thrombosis and vasculitis was also recorded. At 12 and 24 h, minimal inflammatory changes were observed in the contralateral lung. Two weeks after instillation, the right caudal pulmonary lobe had marked chronic inflammatory and fibrosing processes with profound loss of normal parenchymal architecture. In the affected area, alveolar spaces were obliterated by abundant deposition of collagen fibers with interspersed fibroblasts, newly formed blood capillaries, hemosiderin-laden macrophages, and fewer

Table 1. Lung Myeloperoxidase Activity in the Right and Left Lungs

	HCl Treated		NaCl Treated		Baseline	
Time, h	Right (n)	Left (n)	Right (n)	Left (n)	Right (n)	Left (n)
6	86 ± 35 (7)*	88 ± 39 (7)*	88 ± 30 (7)	92 ± 28 (7)	16 ± 4 (4)	15 ± 3 (4)
12	72 ± 19 (9)*	74 ± 37 (9)*	55 ± 18 (7)	45.5 ± 16 (7)		
24	45 ± 21 (7)	27 ± 11 (7)	28 ± 8 (7)	27 ± 9 (76)		

Data are shown as mean ± SD, in units/g wet weight, for mice treated with endobronchial hydrochloric acid (HCl) and saline (NaCl). Numbers in parentheses refer to the number of experiments.

* $P < 0.05$ *vs.* baseline. No significant differences between HCl- and NaCl-treated animals was observed.

lymphocytes (postnecrotic scars). At 2 weeks, no pathologic changes were observed in the contralateral lung.

CT Scan Analysis

Figure 5 shows representative frequency histograms for control and HCl-treated mice at 12 h and 2 weeks from instillation. At 12 h, CT scans analysis revealed greater $CT_{abn,mean}$ and $CT_{abn,w}$ in the HCl group compared with the NaCl group (-39 ± 41 *vs.* -170 ± 105 HU; $P < 0.05$ and 27 ± 16 *vs.* $3 \pm 2\%$; $P < 0.05$). The abnormalities of the HCl group were partially restored at 2 weeks (-179 ± 95 HU; $P < 0.05$ *vs.* HCl at 12 h and $6 \pm 7\%$; $P < 0.05$ *vs.* HCl at 12 h).

Discussion

This study describes a low-mortality murine model of HCl-induced lung injury. We used a selective injury model not only for the high reproducibility of the damage, but also because it allowed the survival of most animals with substantial recovery at 2 weeks. However, the evolution of injury did not achieve complete resolution; rather, the mice showed a persisting impairment of respiratory compliance and evidence of lung fibrosis. The animal mortality for unilateral acid instillation was low (less than 25%), not significantly different from saline controls, and comparable with previous studies.[19] Our model of acid aspiration recapitulated a mild form of acute lung injury characterized by a progressive deterioration of functional lung properties over the first 24 h. In the first 12 h, a major disruption of the normal structure and function of the lung became evident: Oxygenation and compliance decreased and right lung weight increased when compared with the NaCl-treated mice. At 24 h from injury, none of these alterations had recovered, some getting even worse. In contrast with our results, previous studies reported the greatest alteration of the alveolar capillary membrane permeability in earlier phases[7,20–22]; the selective injection of HCl (affecting mainly one of the four lobes of the right lung) might explain this difference. Moreover, some studies of bilateral acid injury suggest that after an initial derangement in lung function, within 4–6 h, there is a second phase of injury around 24 h, at which time cellular influx is maximal and alveolar protein-rich fluid increases again.[23,24] As expected, despite a similar instilled volume, the lung weight of the HCl-treated mice was higher than that of the NaCl-treated mice, with a more pronounced impairment in gas exchange and more evident CT scan alterations; this gives evidence of a permeability damage promoted by HCl rather than a simple volume overload. The CT scan images revealed high-density areas predominantly located in the posterior dependent regions of the lung, where the acid was instilled in supine-lying animals. Therefore, although gas exchange in supine animals reflects the severity and extent of lung injury, it does not necessarily represent the actual gas exchange during spontaneous breathing in prone position.[25] This may contribute to explain the relatively low mortality rate of our model.

Table 2. Peripheral Leukocyte Count per mm^3 of Blood in HCl- and NaCl-treated Mice

Time, h	HCl Group	NaCl Group
6	1,505 ± 401 (5)	1,312 ± 348 (4)
12	2,092 ± 851 (4)*	718 ± 214 (5)
24	848 ± 373 (6)	577 ± 219 (6)

Data are shown as mean ± SD for mice treated with endobronchial hydrochloric acid (HCl) and saline (NaCl). Numbers in parentheses refer to the number of experiments.

* $P < 0.05$ *vs.* NaCl group at the corresponding time point.

Hallmarks of an ongoing inflammatory process were already detectable at 6 h. Indeed, a distinct characteristic of acid induced lung injury is neutrophilic infiltration of the lungs.[8,24,26–28] We confirmed that unilateral acid instillation produces an important neutrophilic infiltration (shown by myeloperoxidase activity in lung tissue and by histologic analysis) both in the injured and in the noninjured lung. The neutrophilic infiltration starts early (at 6 h, and probably before) and persists until 12 h, in keeping with previous studies.[29–31] At 24 h, neutrophilic infiltration was decreased, involving the acid injured lung only.

In agreement with what has been reported,[20,27,31] we found an increase in leukocyte count in the first 12 h, suggesting a systemic response to the focal inflammatory process. Our study confirms that a focal injury often results in infiltration of neutrophils in distant

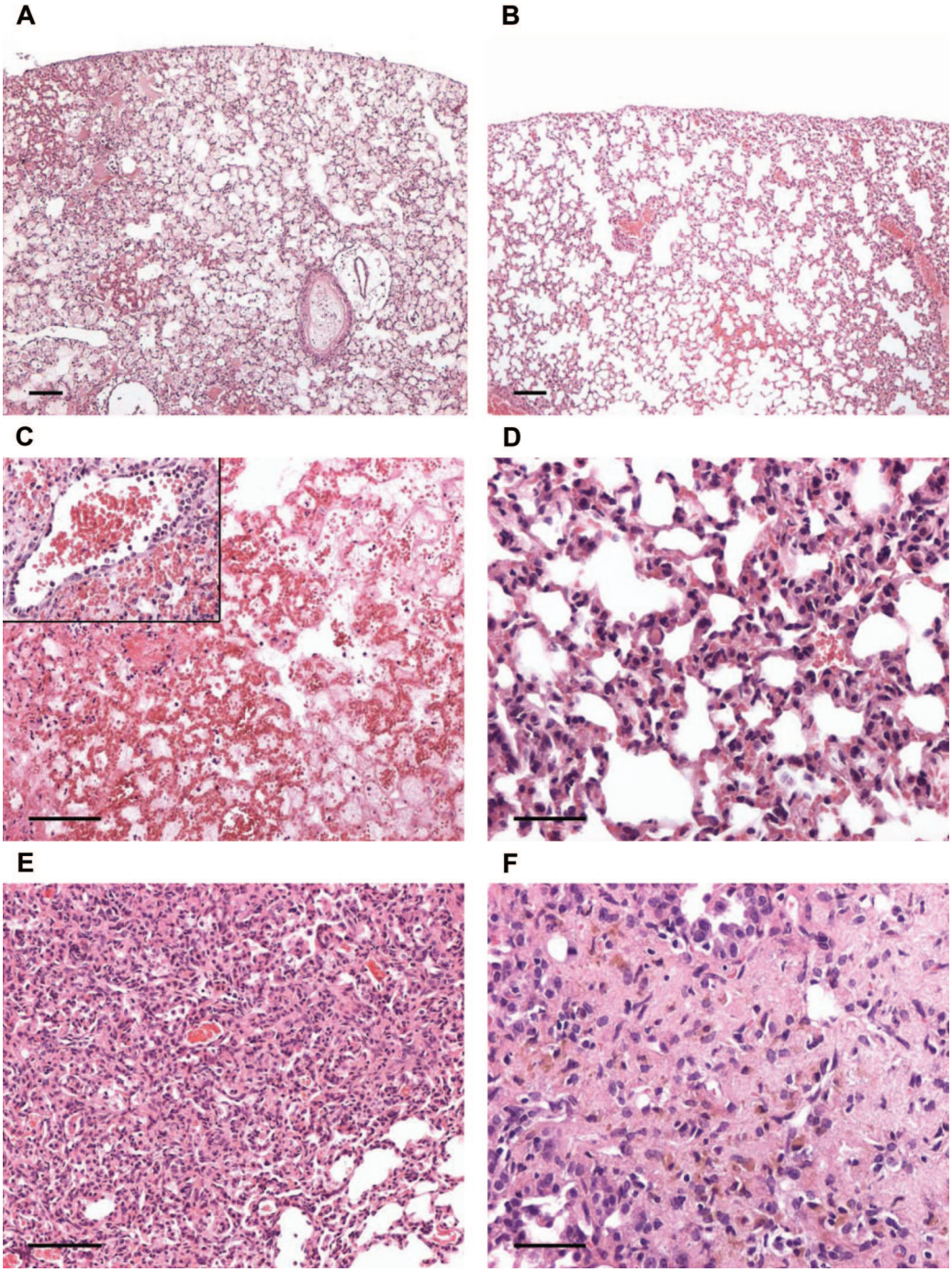

Fig. 4. Representative light micrographs of stained lung tissue sections from hydrochloric acid (HCl)– and saline (NaCl)–treated mice at 12 h, 24 h, and 2 weeks after intrabronchial instillation. (*A*) HCl, 12 h, right lung. Almost all bronchioalveolar spaces are filled by fibrinoproteinaceous material with hyaline membrane formation. Alveolar septa are congested and accompanied by severe interstitial hemorrhages. Notice the medium-sized blood vessels surrounded by a prominent empty halo consistent with severe perivascular edema. Hematoxylin and eosin; *scale bar*, 100 μm. (*B*) NaCl, 12 h, right lung. Instilled lung showed a minimal alveolar septa expansion with sparse neutrophilic infiltrates. Hematoxylin and eosin; *scale bar*, 100 μm. (*C*) HCl, 24 h, right lung. Pulmonary parenchyma is completely effaced by marked necrotic and fibrinohemorrhagic changes associated with severe medium-sized blood vessel thrombosis and vasculitis. The latter finding is characterized by transmural disruption of vascular wall by marked neutrophilic infiltration (*inset*). Hematoxylin and eosin; *scale bar*, 100 μm. (*D*) NaCl, 24 h, right lung. Alveolar septa are moderately expanded with occasional findings of type II pneumocyte reactive hyperplasia. Hematoxylin and eosin; *scale bar*, 50 μm. (*E*) HCl, 2 weeks, right lung. Alveolar spaces are almost completely obliterated by marked alveolar septa fibroplasia accompanied by diffuse type II pneumocyte hyperplasia and mild histioneutrophilic infiltration. Large intraalveolar groups of foamy macrophages are also multifocally evident. Hematoxylin and eosin; *scale bar*, 100 μm. (*F*) HCl, 2 weeks, right lung. Area of scarring showing complete loss of the alveolar architecture due to abundant deposition of collagen fibers with interspersed fibroblast, newly formed blood capillaries, hemosiderin-laden macrophages, and fewer lymphocytes. Hematoxylin and eosin; *scale bar*, 50 μm.

Table 3. Histologic Lung Injury Scores

	Alveolar Serofibrinous Exudate		Alveolar Hemorrhage		Alveolar Inflammatory Cells		Alveolar Septal Thickening		Parenchymal Necrosis		Fibrosis	
Group, Time	HCl	NaCl	HCl	NaCl	HCl	NaCl	HCl	NaCl	HCl	NaCl	HCl	NaCl
Right lung												
6 h	6.0 ± 0.0*	0.5 ± 1.0	3.0 ± 1.2	4.0 ± 5.7	2.0 ± 0.0*	0.8 ± 1.0	3.5 ± 1.0	3.3 ± 6.5	6.0 ± 0.0*	1.0 ± 1.4	0.0 ± 0.0	0.0 ± 0.0
12 h	9.4 ± 4.8*	2.0 ± 3.9	6.4 ± 2.8	2.4 ± 3.8	4.7 ± 2.3*	1.4 ± 2.6	5.9 ± 4.3	4.6 ± 2.3	4.1 ± 3.2*	0.6 ± 1.3	0.0 ± 0.0	0.0 ± 0.0
24 h	18.3 ± 4.9*	0.5 ± 1.0	9.7 ± 0.6*	2.0 ± 4.0	10.7 ± 1.2*	0.3 ± 0.5	5.0 ± 3.6	5.3 ± 7.5	7.7 ± 4.5*	0.0 ± 0.0	0.0 ± 0.0	0.0 ± 0.0
2 wk	1.8 ± 0.5*	0.0 ± 0.0	1.5 ± 1.3	1.2 ± 1.8	6.0 ± 1.6*	0.2 ± 0.5	8.3 ± 3.3	6.0 ± 7.6	2.3 ± 2.9	0.0 ± 0.0	4.0 ± 1.4*	0.0 ± 0.0
Left lung												
6 h	0.0 ± 0.0	0.0 ± 0.0	0.0 ± 0.0	0.0 ± 0.0	0.0 ± 0.0	0.0 ± 0.0	0.0 ± 0.0	0.5 ± 1	0.0 ± 0.0	0.0 ± 0.0	0.0 ± 0.0	0.0 ± 0.0
12 h	0.4 ± 0.8	0.0 ± 0.0	0.4 ± 0.8	0.2 ± 0.5	1.0 ± 1.4	1.1 ± 1.2	1.0 ± 1.0	0.6 ± 0.9	0.1 ± 0.4	0.0 ± 0.0	0.0 ± 0.0	0.0 ± 0.0
24 h	1.0 ± 1.7	0.0 ± 0.0	0.7 ± 1.2	0.3 ± 0.5	0.7 ± 1.2	0.0 ± 0.0	1.0 ± 1.0	0.8 ± 1.0	0.0 ± 0.0	0.0 ± 0.0	0.0 ± 0.0	0.0 ± 0.0
2 wk	0.0 ± 0.0	0.0 ± 0.0	0.0 ± 0.0	0.4 ± 0.9	0.0 ± 0.0	0.0 ± 0.0	0.0 ± 0.0	2.4 ± 3.3	0.0 ± 0.0	0.0 ± 0.0	0.0 ± 0.0	0.0 ± 0.0

The tables summarize the histologic injury scores for the right and left lungs for mice treated with endobronchial hydrochloric acid (HCl) and saline (NaCl) at different time points. Histologic analysis was performed by a semiquantitative scoring system (modified from Carraway *et al.*[17]). An upper, mean, and caudal transversal section of right and left lung for each mouse was evaluated. Six findings were scored for severity and extent of injury. A mean score, expressed as the product of the extent and of the severity, for each finding, zone (upper, mean, caudal), and lung was obtained and is reported in each cell. n = 4–6/group.

* $P < 0.05$ *vs.* NaCl at the same time point.

sites.[27,29,32,33] The increase in myeloperoxidase activity in the contralateral lung could be attributed to circulating mediators release from the site of injury.[29,32]

In addition, in the injured lung, myeloperoxidase activity at 6 h did not differ between the HCl and NaCl groups, as reported in other studies,[21,29] whereas its kinetic in the following period did. In fact, neutrophilic infiltration progressively decreased in the NaCl group, whereas it remained relatively constant in the HCl group. Therefore, our data showed that a relatively large volume of fluid instilled intrabronchially may cause a relevant activation of inflammatory cells that is characterized by a short-term kinetic (particularly in the noninstilled lung) as in the NaCl-treated group. The same volume but with a low pH (<1.5) is responsible for a prolonged neutrophilic lung infiltration.

Hydrochloric acid instillation is known to damage the alveolar epithelium by an early direct chemical burn and by a delayed inflammatory process.[7,8,28] Coagulative necrotic processes developed early after HCl instillation (already present in their maximal extension 6 h after the HCl instillation) and held steady until the 24-h stage. At 6 h after HCl instillation, inflammatory changes were moderate and confined to the perinecrotic area in the caudal right lobe. Later (at 12 and 24 h after HCl instillation), alveolar exudation with hyaline membrane formation and hemorrhage gradually progressed in extension and severity, involving also the medium and the upper right lobes.

The occasional findings of bronchioalveolar suppuration observed in the right lung at 6, 12, and 24 h in the NaCl group could be attributable to early septic complication that took place during right principal bronchus catheterization and NaCl instillation. This finding, which might contribute to explain the mortality rate of the NaCl group, was never detected in HCl-treated mice. A possible explanation for this difference between NaCl and HCl groups is that instilled HCl solution suddenly kills contaminant bacteria and does not allow them to survive and reach the bronchioalveolar junction. Furthermore, it is widely documented that during AP, the low pH of acid gastric content plays a fundamental role in preventing septic complication.[1]

After the first acute exudative phases characterized by the respiratory epithelium damage (particularly of alveolar type I cells), we described a late fibroproliferative phase with activation and proliferation of type II cells to restore the epithelium after injury. Is well known that when the repair process is impaired, it results in the activation and migration of mesenchymal precursor cells (reactive fibroblasts, myofibroblasts, and angioblasts) into the alveolar space with organized granulation tissue formation and progressive fibrosis (fibrosis by accretion).[19,34,35] This process is likely to occur in our model as well; histologic specimens showed injured areas with persistent loss of normal alveolar architecture due to marked fibroplasia and intense collagen deposition 2 weeks after the initial injury. Moreover, at this time point, the animals in the HCl group showed features compatible with a fibrotic evolution of the initial inflammatory process: C_{stat} was reduced, but with a reduction of the right lung wet weight. The presence of a fibrotic scar could finally be confirmed on the CT scan, revealing a reduced but persistent area of abnormal aeration (6% of right lung weight), although less radiologically dense than during the acute phase. This abnormality did not affect lung gas exchange (as indicated by the restored Pa_{O_2}), likely because the area involved was small and/or underperfused. The spontaneous evolution toward fibrosis is a valuable feature of the model because it resembles the spontaneous fibrotic evolution seen on long-term follow-up CT scans in acute lung injury survivors.[36,37] In such patients, however, the fibrosis tended to involve the nondependent lung regions, which were normally aerated in the acute phases of the disease. On the contrary, in our model, the same regions were the site of the acute injury and of the fibrotic evolution. This discrep-

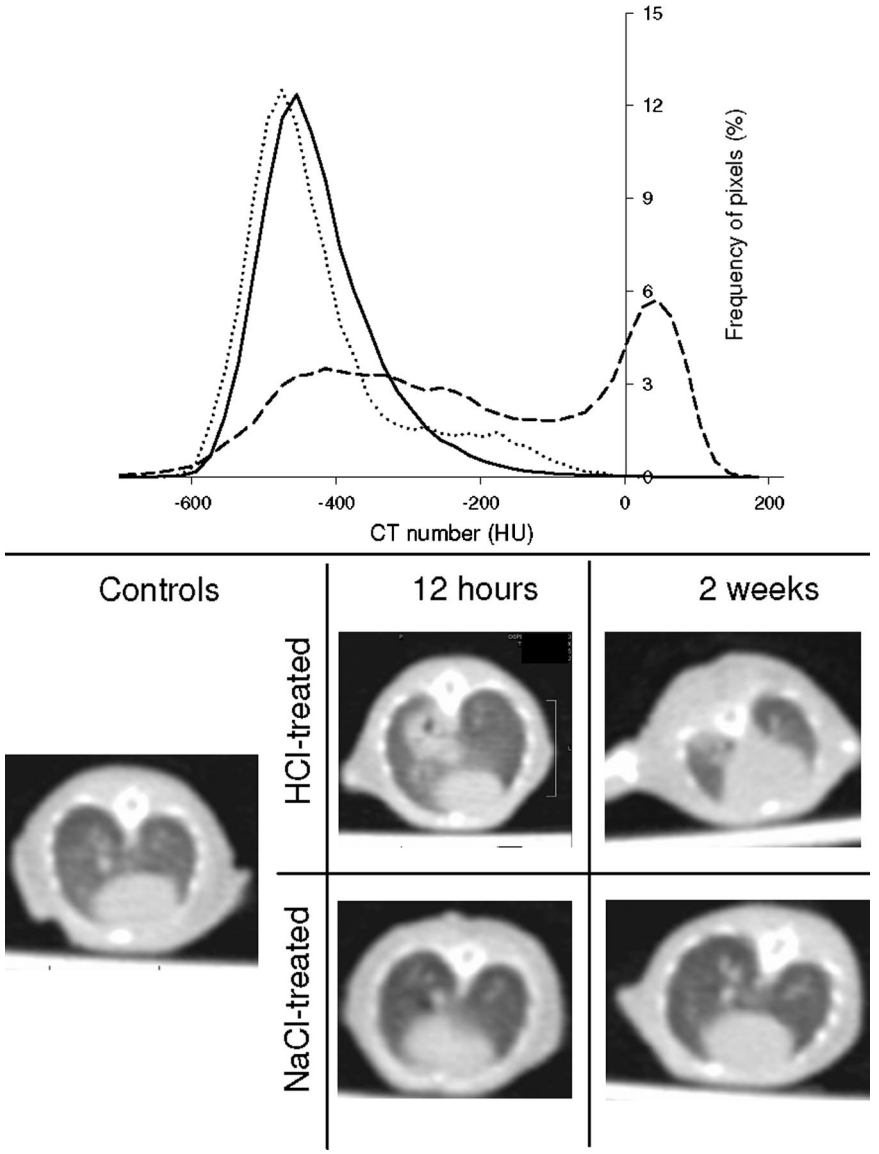

Fig. 5. Frequency histogram for control (*solid line*) and hydrochloric acid (HCl)–treated mice 12 h (*dashed line*) and 2 weeks (*dotted line*) after instillation. The plot represents the relative frequency of the lungs' pixels after dividing them in bins with a width of 20 Hounsfield units (HU). The median value and the frequency distribution for the control mice are similar to what has been reported in studies using a micro–computed tomography (CT). In the distribution of the HCl-treated mice (12 h after instillation) a peak corresponding to the nonaerated parenchyma can be seen, centered approximately around +20 HU, whereas in the 2-week mice, the normal pixel distribution is almost restored. Representative images are shown in the *bottom half* of the figure. In the *left panel*, an untreated scan is shown. Images from HCl-treated and saline (NaCl)–treated mice at both 12 h and 2 weeks are shown in the *central* and *right panels*, respectively. In the HCl-treated mice, an area of aeration loss can be seen in the right lung at 12 h; at 2 weeks, a small area of abnormal aeration can be seen in the dependent zone of the caudal lobe. n = 6–8/group.

ancy could be the result of a milder involvement of the whole lung (as opposed to what happens during acute lung injury) and of the absence of the noxious stimulus represented by mechanical ventilation.

The determinants of evolution toward progressive fibrosis or alveolar recovery after acute lung injury are not entirely understood. Although our long-term injury model could be suitable to investigate the modulation of such a process, we do not provide insights on the mechanisms underlying the observed evolution toward fibrosis. Some studies have suggested a role of activated neutrophils in the scarring process[38] demonstrating that pulmonary fibrosis after lung challenging with fibrogenic and nonfibrogenic inflammatory stimuli correlated with duration of neutrophil activation. Moreover, the role of macrophages in the regulation of pulmonary fibrosis is still under investigation. Once activated, these two cell types can synthesize and release a variety of molecules (*e.g.*, transforming growth factor α, tumor necrosis factor β, platelet-derived growth factor, angiotensin II), which, in adjunction to the activation of the coagulation cascade, promote the fibroproliferative response after acute lung injury.[39–44]

Our study has some limitations that deserve discussion. Although we did not investigate the very early time frames, where a first inflammatory peak has been described, we were more focused on characterizing the evolution of this nonlethal model of acid inspiration, rather than assessing the well-established biphasic pattern of acid instillation.[7] We provide an evaluation of functional and morphologic characteristics of the 2-week sequelae of a unilateral acid instillation, which has not previously been reported except by Yano *et al.*,[19] who only considered the collagen deposition in the lung, at 3 weeks. Moreover, we did not perform an interim analysis between the acute phase and the late one at 2 weeks. We did not perform any dose–response analysis or any evaluation of the effects of cumulative

injuries. However, we used the dose and volume known to cause the largest injury associated with animal survival.[7] The potential interaction between mechanical ventilation and underlying pulmonary injury has been extensively reported.[45,46] We did not explore this aspect because, in our study, mechanical ventilation was limited to maintain animals under anesthesia during the surgical procedure (approximately 10 min). Although we chose an anesthetic agent with a limited risk of interference, anesthesia too could affect the local and systemic response to lung injury.[47]

The use of the small (as opposed to large) animals to develop this model has several advantages, but it might make the results less transferable to other species, including humans. For example, in our model as well as in other mouse models, AP evolution seems to proceed at a slower pace than in rats.[48] The reasons for this difference are not clear. Although they could be the result of a unilateral and selective (rather than diffuse to the whole lung) injury, they are possibly due to different time course or neutrophil dynamics between animal species.[49] The C_{stat} values have been measured for the entire respiratory system and are not specifically referred to the injured lung; however, because in both groups the left lung was only marginally affected, the decrease in compliance observed is likely to reflect (and certainly underestimates) the mechanical impairment of the right lung. The radiologic findings we present were not obtained by a micro-CT scanner designed for small rodents; however, we consider the resolution of our scans as adequate (nominal 0.8 mm): the frequency histogram of CT numbers that we obtained is similar to that given by a micro CT scanner,[18] supporting the adequacy of the human scanner we used.

In conclusion, we characterized several aspects of a murine model of regional acid aspiration allowing long-term animal survival without the need for mechanical ventilation. Interestingly, despite the recovery of endothelial permeability, inflammatory cell infiltration, and gas exchange, at 2 weeks the injury persists, with the formation of a fibrotic scar, which explains the persistent derangement in lung compliance. This long-term, low-mortality model of acid aspiration seems suitable for the assessment of the effects of different therapies[49–51] on lung injury and repair.

The authors thank Eugenio Scanziani, M.D. (Professor, Faculty of Veterinary Medicine, University of Milan, Milan, Italy), for support in histologic result interpretation; Giovanna Balconi, B.Sc. (Head of Tissue Culture Unit, Department of Cardiovascular Research, Istituto di Ricerche Farmacologiche Mario Negri, Milan, Italy), for support and training in peripheral leukocyte counting; and Simona Barlera, M.Sc. (Head of Statistical Unit, Department of Cardiovascular Research, Istituto di Ricerche Farmacologiche Mario Negri), for statistical support.

References

1. Marik PE: Aspiration pneumonitis and aspiration pneumonia. N Engl J Med 2001; 344:665–71

2. Roy TM, Ossorio MA, Cipolla LM, Fields CL, Snider HR, Anderson WH: Pulmonary complications after tricyclic antidepressant overdose. Chest 1989; 96:852–6

3. Warner MA, Warner ME, Weber JG: Clinical significance of pulmonary aspiration during the perioperative period. ANESTHESIOLOGY 1993; 78:56–62

4. Olsson GL, Hallen B, Hambraeus-Jonzon K: Aspiration during anaesthesia: A computer-aided study of 185,358 anaesthetics. Acta Anaesthesiol Scand 1986; 30:84–92

5. Marx GF, Mateo CV, Orkin LR: Computer analysis of postanesthetic deaths. ANESTHESIOLOGY 1973; 39:54–8

6. Lienhart A, Auroy Y, Péquignot F, Benhamou D, Warszawski J, Bovet M, Jougla E: Survey of anesthesia-related mortality in France. ANESTHESIOLOGY 2006; 105:1087–97

7. Kennedy TP, Johnson KJ, Kunkel RG, Ward PA, Knight PR, Finch JS: Acute acid aspiration lung injury in the rat: Biphasic pathogenesis. Anesth Analg 1989; 69:87–92

8. Knight PR, Druskovich G, Tait AR, Johnson KJ: The role of neutrophils, oxidants, and proteases in the pathogenesis of acid pulmonary injury. ANESTHESIOLOGY 1992; 77:772–8

9. Mitsushima H, Oishi K, Nagao T, Ichinose A, Semba M, Iwasaki T, Nagatake T: Acid aspiration induces bacterial pneumonia by enhanced bacterial adherence in mice. Microb Pathog 2002; 33:203–10

10. Ware LB, Matthay MA: The acute respiratory distress syndrome. N Engl J Med 2000; 342:1334–49

11. Zilberberg MD, Epstein SK: Acute lung injury in medical ICU: Comorbid conditions, age, etiology, and hospital outcome. Am J Respir Crit Care Med 1998; 157:1159–64

12. Milberg JA, Davis DR, Steinberg KP, Hudson LD: Improved survival of patients with acute respiratory distress syndrome (ARDS): 1983-1993. JAMA 1995; 273:306–9

13. Rubenfeld GD, Caldwell E, Peabody E, Weaver J, Martin DP, Neff M, Stern EJ, Hudson LD: Incidence and outcomes of acute lung injury. N Engl J Med 2005; 353:1685–93

14. Kozlow JH, Berenholtz SM, Garrett E, Dorman T, Pronovost PJ: Epidemiology and impact of aspiration pneumonia in patients undergoing surgery in Maryland, 1999-2000. Crit Care Med 2003; 31:1930–7

15. Parker JC, Townsley MI: Evaluation of lung injury in rats and mice. Am J Physiol Lung Cell Mol Physiol 2004; 286:L231–46

16. Goldblum SE, Wu KM, Jay M: Lung myeloperoxidase as a measure of pulmonary leukostasis in rabbit. J Appl Physiol 1985; 59:1978–85

17. Carraway MS, Welty-Wolf KE, Miller DL, Ortel TL, Idell S, Ghio AJ, Petersen LC, Piantadosi CA: Blockade of tissue factor. Am J Respir Crit Care Med 2003; 167:1200–9

18. Zhou Z, Kozlowski J, Schuster DP: Physiologic, biochemical, and imaging characterization of acute lung injury in mice. Am J Respir Crit Care Med 2005; 172:344–51

19. Yano T, Deterding RR, Simonet WS, Shanon JM, Mason RJ: Keratinocyte growth factor reduces lung damage due to acid instillation in rats. Am J Respir Cell Mol Biol 1996; 15:433–42

20. Nemzek JA, Call DR, Ebong SJ, Newcomb DE, Bolgos GL, Remik DG: Immunopathology of a two-hit murine model of acid aspiration lung injury. Am J Respir Cell Mol Biol 2000; 278:L512–20

21. Beck-Schimmer B, Rosenberger DS, Neff SB, Jamniki M, Suter D, Fuhrer T, Schwendener R, Booy C, Reyes L, Pasch T, Schimmer RC: Pulmonary aspiration. ANESTHESIOLOGY 2005; 103:556–66

22. Davidson BA, Knight PR, Helinski JD: The role of tumor necrosis factor-α in the pathogenesis of aspiration pneumonitis in rats. ANESTHESIOLOGY 1999; 91:486–99

23. Hagio T, Matsumoto S, Nakao S: Elastase inhibition reduced death associated with acid aspiration-induced lung injury in hamsters. Eur J Pharmacol 2004; 488:173–80

24. Allen GB, Leclair T, Bates JHT: Lung mechanical dysfunction in acid-injured mice fluctuates over first 48 hours. Am J Respir Crit Care Med 2005; 171:A149

25. Richter T, Bellani G, Scott Harris R, Vidal Melo MF, Winkler T, Venegas JG, Musch G: Effects of prone position on regional shunt, aeration, and perfusion in experimental acute lung injury. Am J Respir Crit Care Med 2005; 172:480–7

26. Folkesson HG, Matthay MA, Herbert CA, Broaddus BC: Acid aspiration induced lung injury in rabbits is mediated by interleukin-8-dependent mechanism. J Clin Invest 1995; 111:107–16

27. Goldman G, Werlburn R, Klausener JM, Kobzik L, Valeri CR, Shepro D, Hechtman H: Leukocytes mediate acid aspiration-induced multiorgan edema. Surgery 1992; 114:13–20

28. Weiser MR, Pechet TT, Williams JP, Ma M, Frenette PS, Moore FD, Kobzok L, Hines RO, Wagner DD, Carrol MC, Hechtman HB: Experimental murine acid aspiration injury is mediated by neutrophils and the alternative complement pathway. J Appl Physiol 1997; 83:1090–5

29. Van de Low A, Jean D, Frisdal E, Cerf C, d'Ortho M, Baker AH, Lafuma C, Duvaldestin P, Harf A, Delclaux C: Neutrophil proteinases in hydrochloric acid- and endotoxin-induced acute lung injury: Evaluation of interstitial protease activity by *in situ* zymography. Lab Invest 2002; 82:133–45

30. Fukunada K, Kohli P, Bonnans C, Fredenburgh LE, Levy BD: Cyclooxygen-

ase 2 plays a pivotal role in the resolution of acute lung injury. J Immunol 2005; 174:5033–9

31. Schreiber T, Hueter L, Gaser E, Schmidt B, Schwarzkopf K, Rek H, Karzai W: PEEP has beneficial effects on inflammation in the injured and no deleterious effects on the noninjured lung after unilateral lung acid instillation. Intensive Care Med 2006; 32:740–9

32. Motosugi H, Quinlan WM, Bree M, Doerschuk M: Role of CD11b in focal acid-induced pneumonia and contralateral lung injury in rats. Am J Respir Crit Care Med 1998; 157:192–8

33. Cohen AB, Batra GK: Bronchoscopy and lung lavage induced bilateral pulmonary neutrophils influx and blood leukocytosis in dogs and monkeys. Am Rev Respir Dis 1980; 122:239–47

34. Castro CY: ARDS and diffuse alveolar damage: A pathologist's perspective. Semin Thorac Cardiovasc Surg 2006; 18:13–9

35. Sladen A, Zanca P, Hadnott WH: Aspiration pneumonitis: The sequelae. Chest 1971; 59:448–50

36. Desai SR, Wells AU, Rubens MB, Evans TW, Hansell DM: Acute respiratory distress syndrome: CT abnormalities at long-term follow-up. Radiology 1999; 210:29–35

37. Papazian L, Thomas P, Bregeon F, Garbe L, Zandotti C, Saux P, Gaillat F, Drancourt M, Auffray JP, Gouin F: Open-lung biopsy in patients with acute respiratory distress syndrome. Anesthesiology 1998; 88:935–44

38. Jones HA, Schofield LB, Krausz T, Boobis AR, Haslett C: Pulmonary fibrosis correlates with duration of tissue neutrophils activation. Am J Respir Crit Care Med 1998; 158:620–8

39. Shimabukuro DW, Sawa T, Gropper M: Injury and repair in lung and airways. Crit Care Med 2003; 31:S524–31

40. Prieditis H, Adamson IYR: Alveolar macrophage kinetics and multinucleated giant cell formation after lung injury. J Leukoc Biol 1996; 59:534–8

41. Thannickal VJ, Towes GB, White ES, Lynch JP III, Martinez FJ: Mechanisms of pulmonary fibrosis. Annu Rev Med 2004; 55:395–417

42. Clark JG, Kostal KM, Marino BA: Modulation of collagen production following bleomycin-induced pulmonary fibrosis in hamsters. J Biol Chem 1982; 257:8088–105

43. Adamson IYR, Hedgecock C, Bowden DH: Epithelial cell-fibroblast interactions in lung injury and repair. Am J Pathol 1990; 137:385–92

44. Fukuda Y, Ishizaki M, Masuda Y, Kimura G, Kawanami O, Masugi Y: The role of intraalveolar fibrosis in the process of pulmonary structural remodelling in patients with diffuse alveolar damage. Am J Pathol 1987; 126:171–82

45. Schreiber T, Hueter L, Schwarzkopf K, Hohlstein S, Schmidt B, Karzai W: Increased susceptibility to ventilator-associated lung injury persists after clinical recovery from experimental endotoxemia. Anesthesiology 2006; 104:133–41

46. Choi G, Wolthuis EK, Bresser P, Levi M, Van der Poll T, Dzoljic M, Vroom MB, Schultz MJ: Mechanical ventilation with lower tidal volumes and positive end-expiratory pressure prevents alveolar coagulation in patients without lung injury. Anesthesiology 2006; 105:689–95

47. Reutershan J, Chang D, Hayes JK, Ley K: Protective effects of isoflurane pre-treatment in endotoxin-induced lung injury. Anesthesiology 2006; 104:511–7

48. Allen GB, Leclair T, Cloutier M, Thompson-Figueroa J, Bates JH: The response to recruitment worsens with progression of lung injury and fibrin accumulation in a mouse model of acid aspiration. Am J Physiol Lung Cell Mol Physiol 2007; 292:L1580–9

49. Kavanagh BP, Laffey JG: Hypercapnia: Permissive and therapeutic. Minerva Anestesiol 2006; 72:567–76

50. Spragg R: Surfactant for acute lung injury. Am J Respir Cell Mol Biol 2007; 37:377–8

51. Mathru M, Huda R, Solanki DR, Hays S, Lang JD: Inhaled nitric oxide attenuates reperfusion inflammatory responses in humans. Anesthesiology 2007; 106:275–82